

Improving Signal-to-Noise Ratio Estimation for Autonomous Receivers

M. Simon¹ and S. Dolinar¹

A method by which a popular signal-to-noise ratio (SNR) estimator can be reconfigured to yield improved performance is proposed. The reconfiguration consists of partitioning the symbol interval into a larger (but even) number of subdivisions than the two that have been traditionally suggested for this estimator but still processing the observables in successive pairs. The optimum number of subdivisions is shown to depend on the SNR range in which the true SNR lies; however, we also show that these SNR regions can be significantly widened with very little loss in performance. Most important is the fact that, with this reconfiguration, the SNR estimator tracks the Cramer–Rao bound on the variance of the estimator over the entire range of SNR values.

I. Introduction

Estimation of signal-to-noise ratio (SNR) and providing this estimate to the data detector are essential to the successful functioning of any communications receiver. Depending on the amount of knowledge available on the information-bearing portion of the received signal, a number of such SNR estimators have been discussed in the literature [1–11]. In particular, depending on the application at hand, SNR estimators typically are classified as either “in-service” estimators, i.e., those that derive their estimate in the presence of the unknown data modulation and thus do not impinge on the channel throughput, or those that depend on knowledge of the data sequence and as such require periodical insertion of a training sequence in the data stream in order to function. Although the latter schemes might be expected to yield better performance, they suffer from the fact that periodic insertion of a training sequence reduces the throughput of the system. Aside from knowledge of the data symbols themselves, other factors that potentially affect the choice of SNR estimator are the nature of the modulation itself (i.e., its type and order) and the degree to which knowledge is available of the carrier phase and frequency and to what extent they are compensated for in obtaining the SNR estimate. In the case of autonomous receiver operation, it is desirable to have an SNR estimator that operates successfully in the absence of as much of this additional knowledge as possible.

The split-symbol moments estimator (SSME) [7–12] is a popular in-service SNR estimator whose performance for multiple phase-shift-keying (m -PSK) modulation is invariant to knowledge of the carrier phase, the order m of the modulation, and the data symbols themselves. A block diagram of this estimator

¹ Communications Architectures and Research Section.

The research described in this publication was carried out by the Jet Propulsion Laboratory, California Institute of Technology, under a contract with the National Aeronautics and Space Administration.

is illustrated in Fig. 1. Although ad hoc in nature, this estimator is simple to implement and has a robust performance often approaching that of schemes derived from maximum-likelihood considerations. Originally conceived for binary PSK (BPSK), the SSME makes use of integrations of the received signal plus noise in the first- and second-half subintervals of each data symbol (of total symbol duration T) to form its estimate of signal-to-noise ratio.

The original SSME \tilde{R} for BPSK needed observations of only the in-phase signal component, but a later generalization [10] defined an SSME \hat{R} based on complex-valued samples including both in-phase and quadrature components. The SSME using complex-valued samples was originally developed for an application with BPSK signals but nonzero frequency offset, such that relevant information was present in both in-phase and quadrature components. However, it is easily shown [11] that the SSME \hat{R} using complex-valued samples performs equally well (in terms of the mean and variance of the estimator) for m -PSK independent of the value of m . Specifically, for ideal performance on an additive white Gaussian noise (AWGN) channel, with no frequency uncertainty and perfect symbol timing, the mean and variance are exactly given by [11]

$$E\{\hat{R}\} = R + \frac{R+1}{N-1} \quad (1)$$

$$\text{var}\{\hat{R}\} = \frac{1}{N-2} \left(\frac{N}{N-1}\right)^2 \left[(2+4R) \left(\frac{N-1/2}{N}\right) + R^2 \right]$$

where R is the true symbol SNR and N is the number of data symbols used in forming the estimate.

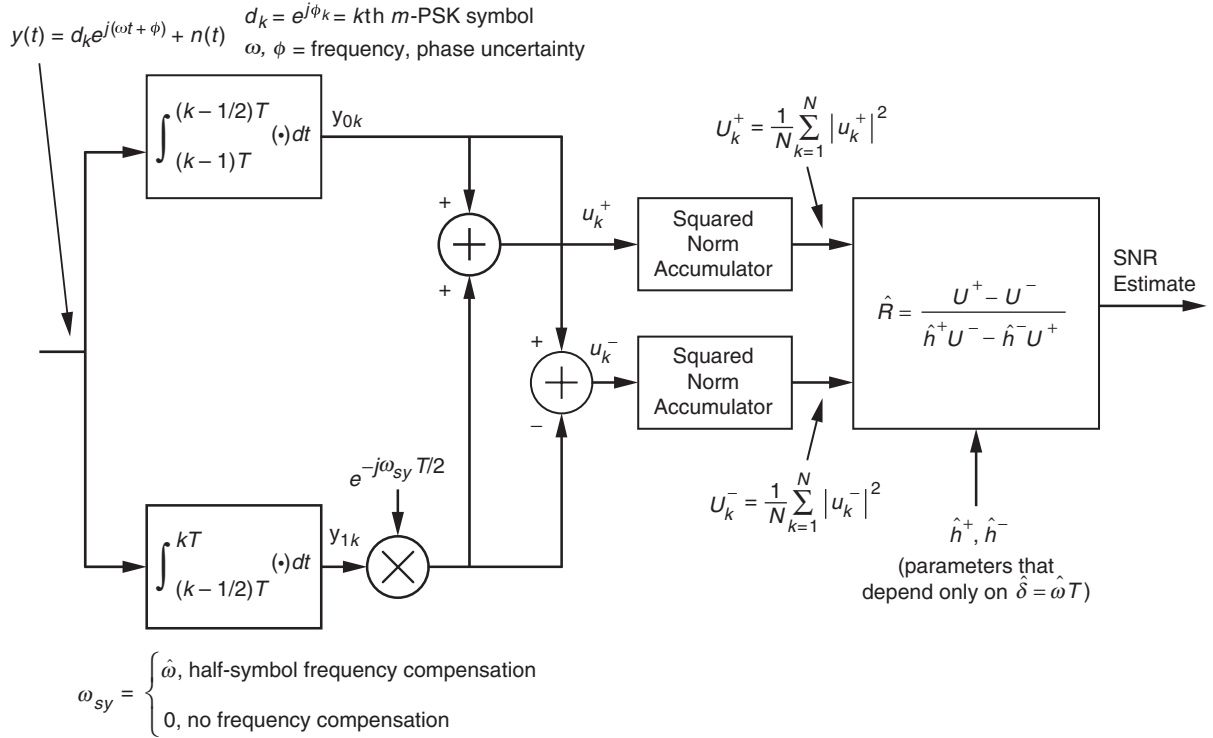


Fig. 1. Split-symbol SNR estimator for m -PSK modulation.

II. A Generalization of the SSME Offering Improved Performance

Now suppose that instead of subdividing each data symbol interval T into two halves, we subdivide it into $2L$ subintervals of equal length $T/2L$ and use the integrations of the complex-valued received signal plus noise in successive pairs of these intervals to form the SNR estimator. In effect, we are estimating the symbol SNR of a data sequence at L times the actual data rate. This data sequence is obtained by repeating each original data symbol to form L consecutive shorter symbols. For a given total observation time (equivalently, a given total number of original symbols N), there are LN short symbols corresponding to the higher data rate, and their symbol SNR is $r = R/L$. Since the SSME is completely independent of the data sequence, the new estimator, denoted by \hat{r}_L , is just an SSME of the SNR $r = R/L$ of the short symbols, based on observing LN short symbols, each split into half. Thus, the mean and variance of \hat{r}_L are computed by simply replacing N with LN and R with R/L in Eq. (1). Since, however, we desire an estimate of R , not $r = R/L$, we define $\hat{R}_L = L\hat{r}_L$ and write the corresponding expressions for the mean and variance of \hat{R}_L :

$$E \left\{ \hat{R}_L \right\} = L \left[\frac{R}{L} + \frac{R/L + 1}{LN - 1} \right] = R + \frac{R + L}{LN - 1} \quad (2)$$

$$\text{var} \left\{ \hat{R}_L \right\} = \frac{L^2}{LN - 2} \left(\frac{LN}{LN - 1} \right)^2 \left[\left(2 + \frac{4R}{L} \right) \left(\frac{LN - 1/2}{LN} \right) + \left(\frac{R}{L} \right)^2 \right]$$

With this notation, the original SSME is simply $\hat{R} = \hat{R}_1$, and the performance expressions in Eq. (2) are valid for any positive integer $L \in \{1, 2, 3, \dots\}$. For large N , i.e., $N \gg 1$, the mean and variance in Eq. (2) simplify within $O(1/N^2)$ to

$$E \left\{ \hat{R}_L \right\} = R + \frac{R + L}{LN} \quad (3)$$

$$\text{var} \left\{ \hat{R}_L \right\} = \frac{L}{N} \left(2 + \frac{4R}{L} + \frac{R^2}{L^2} \right)$$

For the remainder of this section, we base our analytic derivations on the asymptotic expressions in Eq. (3).

For small enough R , we can ignore the R and R^2 terms in the variance expression, and the smallest estimator variance is achieved for $L = 1$. In this case, $\hat{R} = \hat{R}_1$ outperforms (has smaller variance than) \hat{R}_L for $L > 1$, approaching a $10 \log_{10} L$ dB advantage as $R \rightarrow 0$. However, at large enough R for any fixed L , the reverse situation takes place. In particular, retaining only the R^2 term in Eq. (3) for sufficiently large R/L , we see that \hat{R}_L offers a $10 \log_{10} L$ dB advantage over \hat{R} in this limit. This implies that, for small values of R , a half-symbol SSME (i.e., $L = 1$) is the preferred implementation, whereas beyond a certain critical value of R (to be determined shortly), there is an advantage to using values of $L > 1$. In general, for any given R , there is an optimum integer $L = L_*(R)$ that minimizes the variance in Eq. (3). We denote the corresponding optimum estimator by \hat{R}_* . We show below that, unlike the case of the estimator \hat{R}_L defined for a fixed L , the optimized estimator \hat{R}_* requires proportionally more subdivisions of the true symbol interval as R gets large. As a result, the R^2/L^2 term in Eq. (3) does not totally dominate the variance for $R \gg L$, and the amount of improvement at high SNR differs from the $10 \log_{10} L$ dB improvement calculated for an arbitrary fixed choice of L and $R \gg L$.

For the moment we ignore the fact that L must be an integer, and minimize the variance expression in Eq. (3) over continuously varying *real-valued* L . We define an optimum real-valued $L = L_\bullet(R)$, obtained by differentiating the variance expression of Eq. (3) with respect to L and equating the result to zero, as

$$L_{\bullet}(R) = \frac{R}{\sqrt{2}} \quad (4)$$

and a corresponding *fictitious* SNR estimator \hat{R}_{\bullet} that “achieves” the minimum variance calculated by substituting Eq. (4) into the asymptotic variance expression of Eq. (3),

$$\text{var} \left\{ \hat{R}_{\bullet} \right\} = \frac{R}{N} \left(4 + 2\sqrt{2} \right) \quad (5)$$

The minimum variance shown in Eq. (5) can be achieved only by a realizable estimator for values of R that yield an integer $L_{\bullet}(R)$ as defined by Eq. (5). Nevertheless, it serves as a convenient benchmark for comparisons with results corresponding to the optimized realistic implementation \hat{R}_{*} . For example, from Eqs. (3) and (5) we see that the ratio of the asymptotic variance achieved by any given realizable estimator \hat{R}_L to that achieved by the fictitious estimator \hat{R}_{\bullet} is a simple function of the short symbol SNR r , not of R and L separately. In particular,

$$\frac{\text{var} \left\{ \hat{R}_L \right\}}{\text{var} \left\{ \hat{R}_{\bullet} \right\}} = \frac{2/r + 4 + r}{4 + 2\sqrt{2}} \quad (6)$$

The numerator of Eq. (6) is a convex \cup function of r , possessing a unique minimum at $r = \sqrt{2}$, at which point the ratio in Eq. (6) evaluates to unity. This result is not surprising, since from Eq. (4) $r = \sqrt{2}$ is the optimality condition defining the fictitious estimator \hat{R}_{\bullet} . For $r > \sqrt{2}$ or $r < \sqrt{2}$, the ratio in Eq. (6) for any fixed value of L grows without bound.

We return now to the realistic situation where L must be an integer, but can vary with R or r . Since the variance expression in Eq. (3) is convex \cup in L , we can determine whether \hat{R}_L is optimum for a given R by simply comparing its performance to that of its nearest neighbors, \hat{R}_{L-1} and \hat{R}_{L+1} . We find that \hat{R}_L is optimum over a continuous range $R \in [R_L^-, R_L^+]$, where $R_1^- = 0$, $R_{L+1}^- = R_L^+$, and the upper boundary point is determined by equating the variance expressions in Eq. (3) for \hat{R}_L and \hat{R}_{L+1} :

$$R_L^+ = \sqrt{2L(L+1)} \quad (7)$$

Thus, the optimum integer $L_*(R)$ is evaluated as

$$L_*(R) = L, \quad \text{if} \quad \sqrt{2L(L-1)} \leq R \leq \sqrt{2L(L+1)} \quad (8)$$

In particular, we see that \hat{R}_1 is optimum in the region $0 \leq R \leq 2$, implying no improvement over the original SSME for these values of R . For values of R in the region $2 \leq R < 2\sqrt{3}$, one should use \hat{R}_2 (i.e., an estimator based on pairs of quarter-symbol integrations), and in general one should use \hat{R}_L when $\sqrt{2L(L-1)} \leq R \leq \sqrt{2L(L+1)}$. For R in this interval, the improvement factor $I(R)$ (reduction in variance) achieved by the new optimized estimator relative to the conventional half-symbol SSME $\hat{R} = \hat{R}_1$ is calculated as

$$I(R) = \frac{\text{var} \left\{ \hat{R} \right\}}{\text{var} \left\{ \hat{R}_{*} \right\}} = \frac{2 + 4R + R^2}{L \left(2 + \frac{4R}{L} + \frac{R^2}{L^2} \right)}, \quad \sqrt{2L(L-1)} \leq R \leq \sqrt{2L(L+1)} \quad (9)$$

We have already seen that $I(R) = 1$ for R ranging from 0 to 2, whereupon it becomes better to use \hat{R}_2 , allowing $I(R)$ to increase monotonically to a value of $(7 + 4\sqrt{3})/(7 + 4\sqrt{3}) = 1.168$ (equivalent to 0.674 dB) at $R = 2\sqrt{3}$. Continuing on, in the region $2\sqrt{3} \leq R < 2\sqrt{6}$, one should use \hat{R}_3 whereupon $I(R)$ continues to increase monotonically to a value of $(13 + 4\sqrt{6})/(7 + 4\sqrt{6}) = 1.357$ (equivalent to 1.326 dB) at $R = 2\sqrt{6}$. Figure 2 is a plot of $I(R)$ versus R , as determined from Eq. (9). Note that while $I(R)$ is a continuous function of R , the derivative of $I(R)$ with respect to R is discontinuous at the critical values of R , namely, $R = R_L^+$ for $L \in \{1, 2, 3, \dots\}$, but the discontinuity becomes monotonically smaller as L increases.

It is also instructive to compare the performance of the optimized realizable estimator \hat{R}_* with that of the fictitious estimator \hat{R}_\bullet . The corresponding variance ratio is computed directly from Eq. (6), as long as we are careful to delineate the range of validity from Eq. (8), where each integer value of L contributes to the optimized estimator \hat{R}_* :

$$\frac{\text{var}\{\hat{R}_*\}}{\text{var}\{\hat{R}_\bullet\}} = \frac{2/r + 4 + r}{4 + 2\sqrt{2}}, \quad \sqrt{1 - 1/L_*(R)} \leq \frac{r}{\sqrt{2}} \leq \sqrt{1 + 1/L_*(R)} \quad (10)$$

where for the optimized realizable estimator \hat{R}_* the short symbol SNR r is evaluated explicitly in terms of R as $r = R/L_*(R)$. We see that for any value of R the corresponding interval of validity in Eq. (10) always includes the optimal point $r = \sqrt{2}$ at which the ratio of variances is unity. Furthermore, since the width of these intervals (measured in terms of r) shrinks to zero as $L_*(R) \rightarrow \infty$, the ratio of variances makes smaller and smaller excursions from its value of unity at $r = \sqrt{2}$ as $R \rightarrow \infty$, implying $L_*(R) \rightarrow \infty$ from Eq. (8). Thus, the asymptotic performance for large R and large N of the optimized realizable estimator \hat{R}_* is the same as that of the fictitious estimator \hat{R}_\bullet given in Eq. (5). In particular, we see from Eq. (5) that $\text{var}\{\hat{R}_*\}$ grows only linearly in the limit of large R , whereas $\text{var}\{\hat{R}_L\}$ for any fixed L eventually grows quadratically for large enough R/L .

As can be seen from Eq. (3), the generalized SSME \hat{R}_L is asymptotically unbiased (in the limit as $N \rightarrow \infty$). As shown in [11], it is possible to completely remove the bias of the conventional SSME \hat{R} and to define a perfectly unbiased estimator as $\hat{R}^o = \hat{R} - (\hat{R} + 1/N)$. Similarly, we can now define a precisely unbiased version \hat{R}_L^o of our generalized estimator \hat{R}_L by

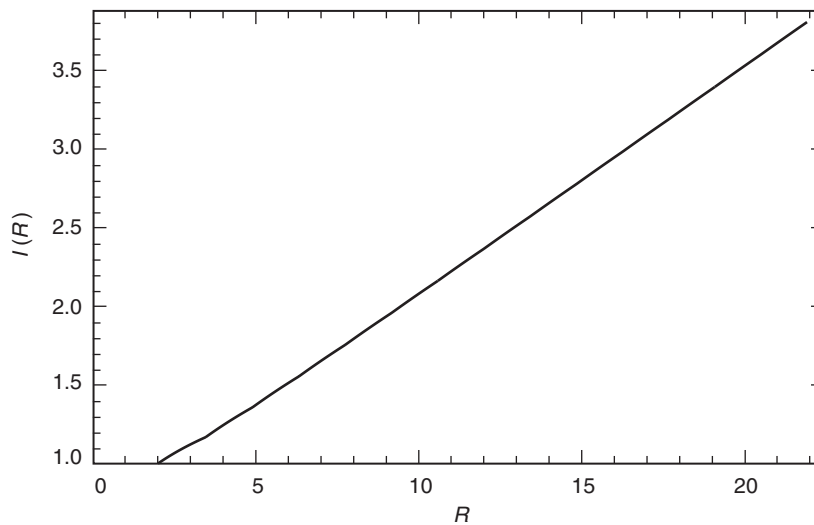


Fig. 2. Performance improvement as a function of SNR.

$$\hat{R}_L^o = \hat{R}_L - \frac{\hat{R}_L + L}{LN} \quad (11)$$

Again we note that the original unbiased SSME \hat{R}^o is just a special case of our generalized unbiased SSME, $\hat{R}^o = \hat{R}_1^o$. Using the Definition (11) together with the expressions in Eq. (2) for the exact mean and variance of \hat{R}_L , we find that the exact mean and variance of the unbiased estimator \hat{R}_L^o are given by

$$\begin{aligned} E \left\{ \hat{R}_L^o \right\} &= R \\ \text{var} \left\{ \hat{R}_L^o \right\} &= \frac{L^2}{LN - 2} \left[\left(1 + \frac{4R}{L} \right) \left(\frac{LN - 1/2}{LN} \right) + \left(\frac{R}{L} \right)^2 \right] \end{aligned} \quad (12)$$

For large N , the asymptotic variance expression obtained from Eq. (12) is identical to that already shown in Eq. (3) for the biased estimator. Thus, all of the preceding conclusions about the optimal choice of L for a given R , and the resulting optimal estimator performance, apply equally to the unbiased versions \hat{R}_L^o of the estimators \hat{R}_L .

III. A Method for Improving the Robustness of the Generalized SSME

For any fixed L , our generalized SSME \hat{R}_L is only optimal when the true SNR R lies in the range $\sqrt{2L(L-1)} \leq R \leq \sqrt{2L(L+1)}$. Indeed, \hat{R}_L for any $L > 1$ is inferior to the original SSME \hat{R}_1 for small enough R (at least for $0 \leq R \leq 2$). The range of optimality for a given value of L , measured in decibels, is just $10 \log_{10} [\sqrt{2L(L+1)}/\sqrt{2L(L-1)}] = 5 \log_{10} [(L+1)/(L-1)]$ dB, which diminishes rapidly toward 0 dB with increasing L . In order to achieve the exact performance of the optimized estimator \hat{R}_* over an unknown range of values of the true SNR R , one would need to select, and then implement, the optimal symbol subdivision based on arbitrarily precise knowledge (measured in decibels) of the very parameter being estimated! Fortunately, there is a more robust version of the generalized SSME that achieves nearly the same performance as \hat{R}_* , yet requires only very coarse knowledge about the true SNR R .

To define the robust generalized SSME, we use the same set of estimators $\{\hat{R}_L\}$ as defined before for any fixed integers L , but now we restrict the allowable choices of L to the set of integers $\{b^\ell, \ell = 0, 1, 2, \dots\}$, for some integer base $b \geq 2$. The optimal choice of L restricted to this set is denoted by $L_{b*}(R)$, and the corresponding optimized estimator is denoted by \hat{R}_{b*} . Because our various estimators differ only in the amount of freedom allowed for the choice of L , their performances are obviously related as

$$\text{var} \left\{ \hat{R}_\bullet \right\} \leq \text{var} \left\{ \hat{R}_* \right\} \leq \text{var} \left\{ \hat{R}_{b*} \right\} \leq \text{var} \left\{ \hat{R}_1 \right\} \quad (13)$$

In this section, we will show analytically that the variance achieved by the robust estimator \hat{R}_{2*} with $b = 2$ comes very close to that achieved by the fictitious estimator \hat{R}_\bullet for all $R \geq 2$, and hence Eq. (13) implies that for this range of R it must be even closer to the less analytically tractable variance achieved by the optimized realizable estimator \hat{R}_* . Conversely, for all $R \leq 2$, we have already seen that the optimized realizable estimator \hat{R}_* is the same as the original SSME \hat{R}_1 , and hence so is the optimized robust estimator \hat{R}_{b*} for any b , since $L = b^0 = 1$ is a permissible value for the robust estimator as well.

The convexity of the general asymptotic variance expression in Eq. (3) again allows us to test the optimality of \hat{R}_{b^ℓ} by simply comparing its performance with that of its nearest permissible neighbors, $\hat{R}_{b^{\ell-1}}$ and $\hat{R}_{b^{\ell+1}}$. The lower and upper endpoints of the region of optimality for any particular \hat{R}_{b^ℓ}

are determined by equating $\text{var}\{\hat{R}_{b^\ell}\}$ with $\text{var}\{\hat{R}_{b^{\ell-1}}\}$ and $\text{var}\{\hat{R}_{b^{\ell+1}}\}$, respectively. This leads to the following definition of the optimal $L_{b^*}(R)$ for L restricted to the set $\{b^\ell, \ell = 0, 1, 2, \dots\}$:

$$L_{b^*}(R) = \begin{cases} b^\ell, & \text{if } \sqrt{2b^{2\ell-1}} \leq R \leq \sqrt{2b^{2\ell+1}} \text{ for integer } \ell \geq 1 \\ b^0 = 1, & \text{if } 0 \leq R \leq \sqrt{2b} \end{cases} \quad (14)$$

For all $R \leq \sqrt{2b}$, the optimized estimator \hat{R}_{b^*} is the same as the original SSME \hat{R}_1 . For all $R \geq \sqrt{2/b}$, the variance achieved by \hat{R}_{b^*} , normalized to that of the fictitious estimator \hat{R}_\bullet , is obtained from Eqs. (6) and (14) in terms of $r = R/L_{b^*}(R)$:

$$\frac{\text{var}\{\hat{R}_{b^*}\}}{\text{var}\{\hat{R}_\bullet\}} = \frac{2/r + 4 + r}{4 + 2\sqrt{2}} \leq \frac{4 + \sqrt{2}(\sqrt{b} + 1/\sqrt{b})}{4 + 2\sqrt{2}}, \quad \frac{1}{\sqrt{b}} \leq \frac{r}{\sqrt{2}} \leq \sqrt{b} \quad (15)$$

As with the earlier expression, Eq. (10), for the variance of \hat{R}_* , the intervals of validity in Eq. (15) for any value of R always include the optimal point $r = \sqrt{2}$ at which the ratio of variances is unity. But unlike Eq. (10), the width of the intervals in Eq. (15) stays constant independent of r . The upper limit on the variance ratio shown in Eq. (15) occurs at the endpoints of these intervals, i.e., for SNR values expressible as $R = \sqrt{2b^{2\ell-1}}$ for some integer $\ell \geq 0$. This upper limit is the maximum excursion from unity of the variance ratio for all $R \geq \sqrt{2/b}$. For all $R \leq 2$ and any $b \geq 2$, there is no limit on the suboptimality of \hat{R}_{b^*} with respect to the fictitious estimator \hat{R}_\bullet , but in this range, \hat{R}_{b^*} suffers no suboptimality with respect to the optimized realizable estimator \hat{R}_* , since both are equivalent to the original SSME \hat{R}_1 for $R \leq 2$. Finally, reiterating our earlier conclusion based on the simple inequalities in Eq. (13), we conclude that the maximum degradation $D(R)$ of the robust estimator \hat{R}_{b^*} with respect to the optimized realizable estimator \hat{R}_* is upper bounded for all R by

$$D(R) = \frac{\text{var}\{\hat{R}_{b^*}\}}{\text{var}\{\hat{R}_*\}} \leq \frac{\text{var}\{\hat{R}_{b^*}\}}{\text{var}\{\hat{R}_\bullet\}} \leq \frac{4 + \sqrt{2}(\sqrt{b} + 1/\sqrt{b})}{4 + 2\sqrt{2}} \quad \text{for all } R \quad (16)$$

For example, we consider the case of $b = 2$, which yields permissible values of L given by $L = 1, 2, 4, 8, 16, \dots$ and corresponding decision region boundaries at $R = 1, 2, 4, 8, 16, \dots$, i.e., regions separated by 3 dB. From Eq. (16), the maximum degradation D_{\max} for using the coarsely optimized estimator \hat{R}_{2^*} instead of the fully optimized realizable estimator \hat{R}_* is no more than

$$D_{\max} \leq \frac{7}{4 + 2\sqrt{2}} = 1.02513 \quad (17)$$

i.e., a penalty of only 2.5 percent. Even if we were to enlarge the regions of constant $L_{b^*}(R)$ to a width of 9 dB in R (corresponding to $b = 8$), the maximum penalty would only increase to

$$D_{\max} \leq \frac{8.5}{4 + 2\sqrt{2}} = 1.245 \quad (18)$$

i.e., a penalty just under 25 percent. Thus, even though the optimized generalized SSME \hat{R}_* requires (in principle) very precise prior knowledge of the true value of R , its performance can be reasonably well approximated by that of a robust estimator \hat{R}_{b^*} requiring only a very coarse prior estimate of R .

IV. Special Case of the SSME for BPSK-Modulated Data

We can define an analogous sequence of generalized SSMEs $\{\tilde{R}_L, L = 1, 2, \dots\}$ corresponding to the original SSME $\tilde{R} = \tilde{R}_1$ developed for BPSK signals using real-valued in-phase samples only. In this case, the (exact) mean and variance of the original SSME \tilde{R} are given by [9]

$$E\{\tilde{R}\} = R + \frac{2R+1}{N-2}$$

$$\text{var}\{\tilde{R}\} = \frac{1}{N-4} \left(\frac{N}{N-2}\right)^2 \left[(1+4R) \left(\frac{N-1}{N}\right) + 2R^2 \right]$$
(19)

The mean and variance of the generalized SSME \tilde{R}_L based on real-valued samples are obtained from Eq. (19) by following the same reasoning that led to Eq. (2):

$$E\{\tilde{R}_L\} = L \left[\frac{R}{L} + \frac{2R/L+1}{LN-2} \right] = R + \frac{2R+L}{LN-2}$$

$$\text{var}\{\tilde{R}_L\} = \frac{L^2}{LN-4} \left(\frac{LN}{LN-2}\right)^2 \left[\left(1 + \frac{4R}{L}\right) \left(\frac{LN-1}{LN}\right) + 2\left(\frac{R}{L}\right)^2 \right]$$
(20)

and the asymptotic forms for large N , i.e., $N \gg 1$, are within $O(1/N^2)$ of

$$E\{\tilde{R}_L\} = R + \frac{2R+L}{LN}$$

$$\text{var}\{\tilde{R}_L\} = \frac{L}{N} \left[1 + 4\left(\frac{R}{L}\right) + 2\left(\frac{R}{L}\right)^2 \right]$$
(21)

We can argue as in [10] that the first- and second-order statistics of the SSME \hat{R}_L based on complex samples are derivable from those of the SSME \tilde{R}_L based on real samples. Specifically, since \hat{R}_L is obtained from twice as many real observables as \tilde{R}_L , with (on average) only half the SNR (since the SNR is zero in the quadrature component for BPSK signals), we have the following (exact) equalities:

$$E\left\{\frac{\hat{R}_L}{2}\right\}_{(R,N)} = E\{\tilde{R}_L\}_{\left(\frac{R}{2}, 2N\right)}$$

$$\text{var}\left\{\frac{\hat{R}_L}{2}\right\}_{(R,N)} = \text{var}\{\tilde{R}_L\}_{\left(\frac{R}{2}, 2N\right)}$$
(22)

where now we have explicitly denoted the dependence of \hat{R}_L and \tilde{R}_L on the SNR and the number of symbols. The equalities in Eq. (22) can be verified by direct comparison of Eq. (20) with Eq. (2) and Eq. (21) with Eq. (3).

As in our earlier analysis of the generalized SSME \hat{R}_L based on complex-valued samples, we can also optimize the generalized SSME \tilde{R}_L based on real-valued samples with respect to its asymptotic

performance expressions in Eq. (21). We define for any fixed value of R an optimum integer $L = \tilde{L}_*(R)$ and an optimum real number $L = \tilde{L}_\bullet(R)$ to minimize the asymptotic variance expression in Eq. (21), and corresponding optimal realizable and fictitious estimators \tilde{R}_* and \tilde{R}_\bullet . For the optimum realizable estimate we find, corresponding to Eq. (8), that the optimum integer $\tilde{L}_*(R)$ is evaluated as

$$\tilde{L}_*(R) = L, \quad \text{if } \sqrt{L(L-1)/2} \leq R \leq \sqrt{L(L+1)/2} \quad (23)$$

We find, corresponding to Eqs. (4) and (5), that the optimal real value of L is $\tilde{L}_\bullet(R) = R\sqrt{2}$ and the corresponding variance is

$$\text{var} \left\{ \tilde{R}_\bullet \right\} = \frac{R}{N} \left(4 + 2\sqrt{2} \right) = \text{var} \left\{ \hat{R}_\bullet \right\} \quad (24)$$

In other words, the fictitious estimator achieves identical variance using either real samples or complex samples.

Finally, we observe from a comparison of Eqs. (2) and (20) an interesting (exact) relationship between the means and variances of the two generalized SSMEs for different values of the symbol rate oversampling factor L :

$$\begin{aligned} E \left\{ \hat{R}_L \right\} &= E \left\{ \tilde{R}_{2L} \right\} \\ \text{var} \left\{ \hat{R}_L \right\} &= \text{var} \left\{ \tilde{R}_{2L} \right\} \end{aligned} \quad (25)$$

Thus, the estimators \tilde{R}_L based on real samples can be viewed as a more finely quantized sequence than the estimators \hat{R}_L based on complex samples, in that any mean and variance achievable by an estimator in the latter sequence is also achievable by taking twice as many subintervals in a corresponding estimator from the former sequence. This implies, for example, that the maximum deviation of the variances of \tilde{R}_* and \tilde{R}_\bullet is no greater than that calculated in Eq. (10) for the deviation between the variances of \hat{R}_* and \hat{R}_\bullet .

V. Comparison with the Cramer–Rao Lower Bound on the Variance of SNR Estimators

A good benchmark for the performance of a given SNR estimator is the Cramer–Rao (C-R) lower bound on its variance [12]. Here we present for comparison the C-R lower bound for any SNR estimator using a given number of observables (samples) per symbol interval, with or without knowledge of the data. For simplicity, we consider only estimators based on real observables, since a number of C-R bounds reported elsewhere [2,6,13] have explicitly considered that case.

It has been shown in [13] that the C-R lower bound on the variance of an arbitrary unbiased estimator of SNR, R^* , in the presence of unknown binary equiprobable data and M independent real observations per symbol (M subinterval samples) is given by

$$\text{var} \{ R^* \} \geq \frac{2R^2}{N} \left[\frac{2M + 2R - E_2(2R)}{2MR - (4R + M)E_2(2R)} \right] \quad (26)$$

where

$$E_2(2R) = E\{X^2 \text{sech}^2 X\} \quad (27)$$

with X a Gaussian random variable with mean and variance both equal to $2R$. The expectation in Eq. (27), which depends only on R , cannot be determined in closed form but is easily evaluated numerically. Figure 3 (discussed at the end of this section) compares the C-R bounding variance in Eq. (26) with the actual asymptotic variance in Eq. (21) achieved by the generalized SSME \tilde{R}_L based on real samples. For this comparison, we substitute $M = 2L$ in the C-R bound expression (because there are $M = 2L$ subinterval integrations contributing to the SSME \tilde{R}_L), and we plot the cases $L = 1, 2, 4, \infty$.

We can also perform analytic comparisons in the limits of low and high SNR. The low- and high-SNR behavior of the C-R bounding variance in Eq. (26) is given by [13]

$$\text{var}\{R^*\} \geq \begin{cases} \frac{1}{2N} \left(\frac{M}{M-1} \right), & R \ll 1 < M \\ \frac{2R}{N} \left(1 + \frac{R}{M} \right), & R \gg M \end{cases} \quad (28)$$

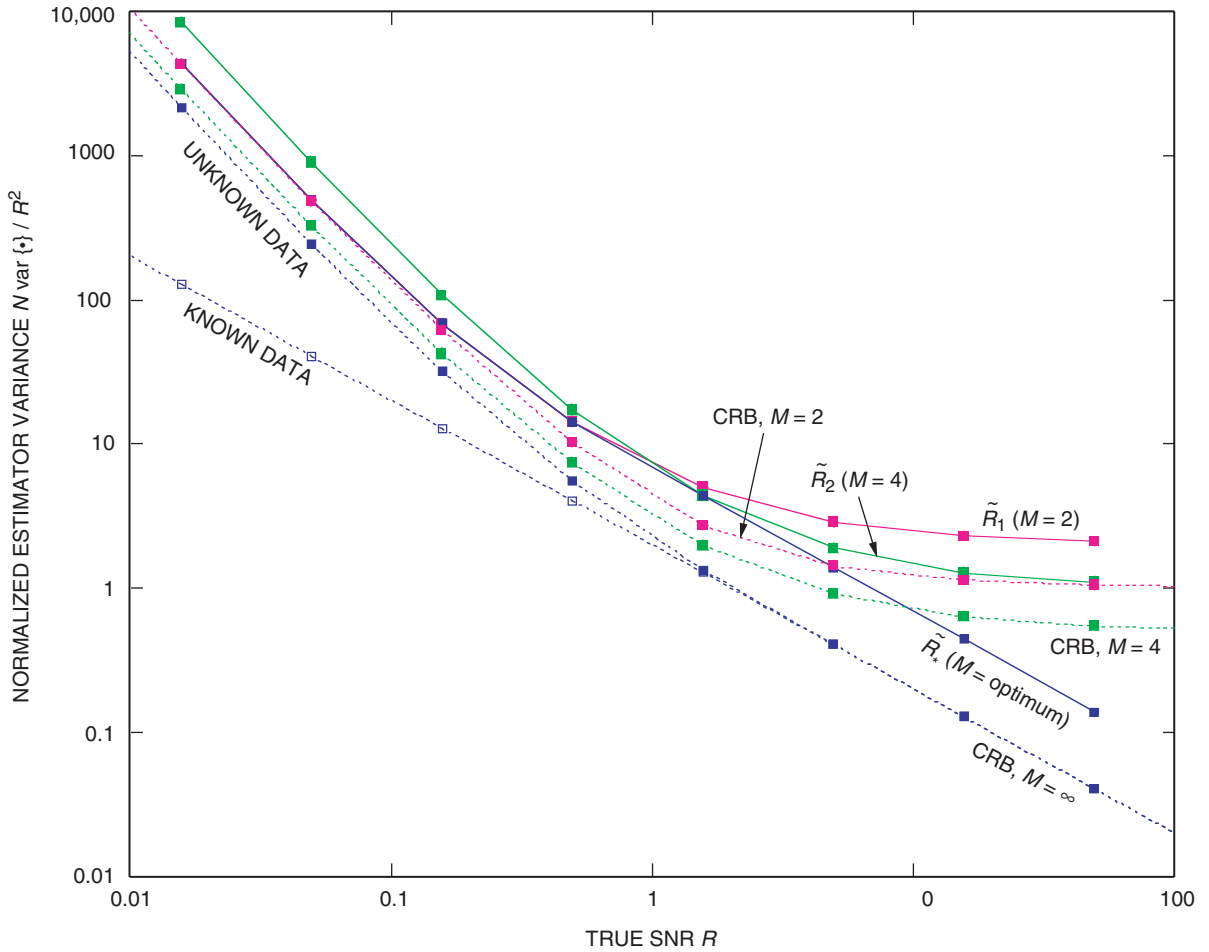


Fig. 3. Comparison of the performance of several SNR estimators with the Cramer–Rao bound.

By comparison, the asymptotic expression in Eq. (21) for the variance of \tilde{R}_L for any fixed L reduces in the low and high SNR limits to

$$\text{var} \left\{ \tilde{R}_L \right\} \approx \begin{cases} \frac{L}{N} = \frac{M}{2N}, & L \gg R \\ \frac{2R^2}{NL} \left(1 + \frac{2L}{R} \right) = \frac{4R}{N} \left(1 + \frac{R}{M} \right), & R \gg L \end{cases} \quad (29)$$

Compared to the C-R bounding variance in Eq. (28), the actual variance in Eq. (29) is higher by a factor of $M - 1$ in the low-SNR limit and by a factor of 2 in the high-SNR limit.

For any fixed M , the C-R bounding variance in Eq. (26) becomes quadratic in R as R approaches infinity, as evidenced by the second expression in Eq. (29). On the other hand, the limiting behavior of the bound for M approaching infinity with fixed R is given by

$$\text{var} \{R^*\} \geq \frac{1}{N} \left[\frac{4R^2}{2R - E_2(2R)} \right], \quad M \gg \max(R, 1) \quad (30)$$

Since $E_2(2R) \approx 2R + 8R^2 + O(R^3)$ for small R and is exponentially small for large R [13], the C-R bounding variance on the right side of Eq. (30) approaches a constant at low SNR and becomes linear in R at high SNR:

$$\text{var} \{R^*\} \geq \begin{cases} \frac{1}{2N}, & M \gg 1 \gg R \\ \frac{2R}{N}, & M \gg R \end{cases} \quad (31)$$

Since the C-R bounding expressions in Eqs. (30) and (31) for large values of $M = 2L$ reflect the best possible performance of an estimator with access to a continuum of samples within each symbol, they are suitably compared to the performance of the optimized estimator \tilde{R}_* , rather than to the performance of \tilde{R}_L for any fixed L . As an approximation to \tilde{R}_* , we use a stand-in estimator equal to \tilde{R}_1 for $R \leq 2$ (i.e., where $\tilde{L}_*(R) = 1$) and to the fictitiously optimized estimator \tilde{R}_\bullet for $R > 2$. The corresponding asymptotic variances computed from Eq. (21) for the limits corresponding to those in Eq. (31) are

$$\begin{cases} \text{var} \left\{ \tilde{R}_1 \right\} = \frac{1}{N}, & 1 \gg R \\ \text{var} \left\{ \tilde{R}_\bullet \right\} = \frac{R}{N} (4 + 2\sqrt{2}), & R \gg 1 \end{cases} \quad (32)$$

The estimator variances in Eq. (32) are higher than the corresponding C-R bounding variances in Eq. (31) by a factor of 2 in the low-SNR limit and by a factor of $2 + \sqrt{2} \approx 3.4$ in the high-SNR limit. The optimized *realizable* estimator \tilde{R}_* suffers an additional small suboptimality factor with respect to the performance of the fictitious estimator \tilde{R}_\bullet used as its stand-in in Eq. (32).

Finally, we consider for purposes of comparison the C-R bound on an arbitrary unbiased estimator when the data are perfectly known. The C-R bound under this assumption is well known [e.g., A, B, C]. Here we continue with the notation of [13] by noting that the derivation there for the case of unknown data is easily modified to the known-data case by skipping the average over the binary equiprobable data. The result is equivalent to replacing the function $E_2(2R)$ by zero in the C-R bound expression in Eq. (26), i.e.,

$$\text{var} \left\{ \hat{R} \right\} \geq \frac{2R^2}{N} \left[\frac{2M + 2R}{2MR} \right] = \frac{2R}{N} \left(1 + \frac{R}{M} \right), \quad \text{for all } M, R \quad (33)$$

Comparing this bound for known data, which is valid for all M and R , with the high-SNR bound for the unknown data case as given in the second expression in Eq. (28), we see that the two variance expressions are identical (to within the approximation that $E_2(2R)$ is exponentially small for large R). Thus, we reach the interesting and important conclusion that, based on the C-R bounds, *knowledge of the data is inconsequential in improving the accuracy of an optimized SNR estimator at high enough SNR!* Conversely, at low SNR, we have seen in Eq. (28) that the C-R bounding variance for the case of unknown data hits a nonzero floor at $(1/2N)[M/(M-1)]$ no matter how closely R approaches zero, whereas the bounding variance in Eq. (33) for the case of known data goes to zero linearly in R . Thus, knowledge of the data fundamentally changes the behavior of the C-R bound at low SNR, and it can be quite helpful in this region for improving the accuracy of the estimator.

Figure 3 summarizes the comparisons of our generalized SSME with the relevant C-R bounds (CRB). This figure plots CRB as a function of true SNR R , for $M = 2, 4, \infty$ with unknown data, and for $M = \infty$ with known data. Also shown for comparison are the actual asymptotic variances achieved by the original SSME \tilde{R}_1 , the generalized SSME \tilde{R}_2 using four subinterval integrations within each symbol, and the optimized generalized SSME \tilde{R}_* . In each case, the asymptotic variance is plotted in normalized form as $N\text{var}\{\cdot\}/R^2$, which can be interpreted as the number of symbols N that must be observed to achieve a *fractional* estimator variance of 100 percent; smaller fractional variances require inversely proportionately larger numbers of symbols.

VI. Improvement in the Presence of Frequency Uncertainty

In [11] the authors considered the performance of the conventional ($L = 1$) SSME in the presence of carrier phase and frequency uncertainties. A variety of cases were considered, corresponding to the degree to which the frequency uncertainty is estimated and compensated for. Here we extend the results given there to the scenario under investigation, i.e., we examine the improvement in performance when frequency uncertainty is present, obtained by optimally partitioning the symbol interval in accordance with the value of the true SNR. In the case where the frequency uncertainty is not estimated, one has no choice other than to use the SNR boundaries determined in the no-frequency-uncertainty case, i.e., those given in Eq. (8) or Eq. (14). For the cases where an estimate of the frequency uncertainty is available, and therefore can be compensated for, one can use this information, if desired, to modify the SNR boundaries. However, to a first-order approximation, we shall assume in what follows that we always determine the boundaries for the symbol regions of fixed partitioning from their zero-frequency-uncertainty values. This allows one to implement a fixed SSME configuration independent of the knowledge of the frequency error and yet still obtain the possibility of a performance advantage relative to the conventional half-symbol split structure. To illustrate the application of the principles involved and resulting performance gains obtained, we shall consider a few of the cases treated in [11].

A. Case 1: Frequency Uncertainty, No Frequency Estimation (and thus No Phase Compensation)

For this case, it was shown in [11] that the variance of the conventional SSME is given by

$$\begin{aligned} \text{var} \{ \hat{R} \} &= \left(\frac{N}{N-1} \right)^2 \left\{ \left(\frac{N-1}{N-2} \right) \left[\frac{(1+2h^+(\delta)R)}{N} + (1+h^+(\delta)R)^2 \right] \right. \\ &\quad \left. \times {}_1F_1(2; N; -Nh^-(\delta)R) - (1+h^+(\delta)R)^2 [{}_1F_1(1; N; -Nh^-(\delta)R)]^2 \right\} \end{aligned} \quad (34)$$

where ${}_1F_1(a; b; z)$ is the Kummer confluent hypergeometric function and

$$h^\pm(\delta) \triangleq \text{sinc}^2 \left(\frac{\delta}{4} \right) \left[\frac{1 \pm \cos(\delta/2)}{2} \right] \quad (35)$$

with $\delta \triangleq \omega T$ denoting the normalized (to the symbol time) frequency uncertainty. Note that in the absence of frequency uncertainty, i.e., $\delta = 0$, using the fact that ${}_1F_1(a; b; 0) = 1$, it is straightforward to show that Eq. (34) simplifies to Eq. (1) as it should.

To modify the expression in Eq. (34) for the case of $2L$ partitions of the symbol interval, we proceed as before by replacing R with R/L , N with LN , δ with δ/L , and then multiplying the result by L^2 resulting in

$$\begin{aligned} \text{var} \{ \hat{R}_L \} &= L^2 \left(\frac{LN}{LN-1} \right)^2 \left\{ \left(\frac{LN-1}{LN-2} \right) \left[\frac{\left(1 + 2h^+(\delta/L) \frac{R}{L} \right)}{LN} + \left(1 + h^+(\delta/L) \frac{R}{L} \right)^2 \right] \right. \\ &\quad \left. \times {}_1F_1(2; LN; -Nh^-(\delta/L)R) - \left(1 + h^+(\delta/L) \frac{R}{L} \right)^2 [{}_1F_1(1; LN; -Nh^-(\delta/L)R)]^2 \right\} \end{aligned} \quad (36)$$

Then, the improvement in performance is obtained by taking the ratio of Eq. (34) to Eq. (36), i.e.,

$$I(R) = \frac{\text{var} \{ \hat{R} \}}{\text{var} \{ \hat{R}_L \}} \quad (37)$$

where, for a value of R in the interval $R_L^- \leq R < R_L^+$, the value of L to be used corresponds to that determined from Eq. (8) or alternatively from Eq. (14). We note that since the boundaries of the SNR regions of Eqs. (8) and (14) are determined from the asymptotic (large N) expressions for the estimator variance, a plot of $I(R)$ versus R determined from Eq. (37) will exhibit small discontinuities at these boundaries. These discontinuities will become vanishingly small as N increases.

Figures 4 and 5 illustrate such a plot for values of N equal to 20 and 100, respectively, with δ as a parameter. We make the interesting observation that although on an absolute basis the variance of the

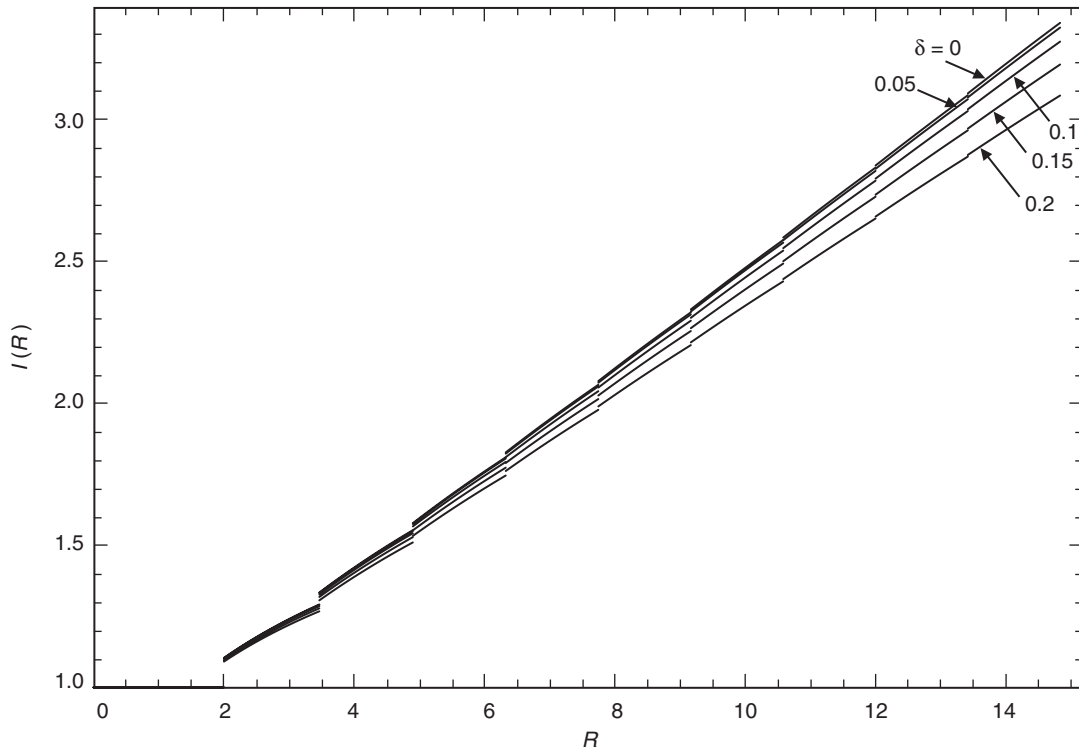


Fig. 4. Improvement factor versus SNR with normalized frequency uncertainty as a parameter; Case 1; $N = 20$.

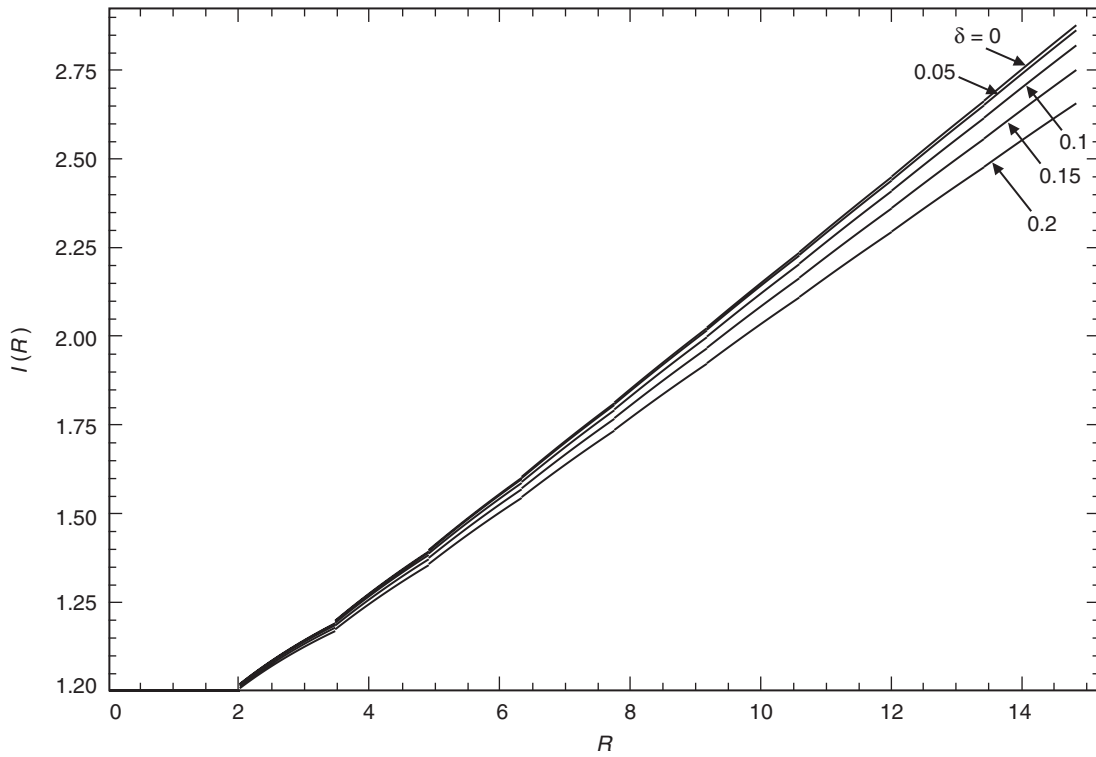


Fig. 5. Improvement factor versus SNR with normalized frequency uncertainty as a parameter; Case 1; $N = 100$.

estimator monotonically improves with increasing N , the improvement factor as evaluated from Eq. (37), which makes use of the exact expression for the estimator variance, shows a larger improvement for smaller values of N . To see how this comes about analytically, we examine the behavior of the zero-frequency-uncertainty improvement factor for large SNR. For sufficiently large SNR (equivalently, large L), we obtain from Eq. (2) the same asymptotic expression as given in Eq. (3) when assuming N large. Also, since for large SNR L and R are approximately related by $L = R/\sqrt{2}$, then substituting this in Eq. (3) gives the asymptotic result

$$\text{var} \left\{ \hat{R}_L \right\} \cong \frac{R}{N} \left(4 + 2\sqrt{2} \right) \quad (38)$$

From Eq. (1), we have for sufficiently large SNR

$$\text{var} \left\{ \hat{R} \right\} = \frac{1}{N-2} \left(\frac{N}{N-1} \right)^2 R^2 \quad (39)$$

Thus, the improvement factor for large SNR is the ratio of Eq. (39) to Eq. (38), namely,

$$I(R) = \frac{\frac{1}{N-2} \left(\frac{N}{N-1} \right)^2 R^2}{\frac{R}{N} \left(4 + 2\sqrt{2} \right)} = \frac{R}{4 + 2\sqrt{2}} \left(\frac{N}{N-2} \right) \left(\frac{N}{N-1} \right)^2 \quad (40)$$

which, for a given R , is a monotonically decreasing function of N approaching $I(R) = R/(4 + 2\sqrt{2})$ in the limit as $N \rightarrow \infty$.

B. Case 2b: Frequency Uncertainty, Perfect Frequency Estimation, Fractional-Symbol Phase Compensation

Another interesting case corresponds to the situation where the frequency uncertainty is perfectly estimated and then used to compensate for the phase shift caused by this uncertainty in the second half of the symbol interval. For this case, the variance of the estimator was determined in [11] as

$$\text{var} \left\{ \hat{R} \right\} = \frac{1}{(h^+(\delta))^2} \frac{1}{N-2} \left(\frac{N}{N-1} \right)^2 \left[\left(1 + 2h^+(\delta)R \right) \left(\frac{2N-1}{N} \right) + (h^+(\delta)R)^2 \right] \quad (41)$$

where now

$$h^+(\delta) \triangleq \text{sinc}^2 \left(\frac{\delta}{4} \right) \quad (42)$$

Making the same substitutions as before, for a $2L$ -partition of the symbol interval we obtain

$$\begin{aligned} \text{var} \left\{ \hat{R}_L \right\} = L^2 \frac{1}{(h^+(\delta/L))^2} \frac{1}{LN-2} \left(\frac{LN}{LN-1} \right)^2 & \left[\left(1 + 2h^+ \left(\frac{\delta}{L} \right) \frac{R}{L} \right) \left(\frac{2LN-1}{LN} \right) \right. \\ & \left. + \left(h^+ \left(\frac{\delta}{L} \right) \frac{R}{L} \right)^2 \right] \end{aligned} \quad (43)$$

Comparing Eq. (41) with Eq. (1), we observe that, in this case, the variance of $h^+(\delta)\hat{R}$ for the conventional SSME is identical to the variance of \hat{R} in the zero-frequency-uncertainty case. From a comparison of Eqs. (43) and (2), a similar equivalence can be made between the variance of $h^+(\delta/L)\hat{R}$ and the variance of \hat{R} for the $2L$ -partition estimator.

Analogous to what was done for Case 1, the improvement factor, $I(R)$, here can be obtained from the ratio of Eq. (41) to Eq. (43). Figures 6 and 7 are plots of $I(R)$ versus true SNR, R , for values of N equal to 20 and 100, respectively, with δ as a parameter. Once again we make the observation that a larger improvement is obtained for smaller values of N . An analytical justification for this observation can be demonstrated by examining the behavior of I for large SNR. Specifically, the analogous expression to Eq. (40) now becomes

$$I(R) = \frac{\left(\frac{1}{(h^+(\delta))^2 R} + \frac{2}{h^+(\delta)}\right) \left(\frac{2N-1}{N}\right) + R}{\frac{4}{h^+(\sqrt{2}\delta/R)} + \sqrt{2} \left(1 + \frac{1}{(h^+(\sqrt{2}\delta/R))^2}\right)} \left(\frac{N}{N-2}\right) \left(\frac{N}{N-1}\right)^2 \quad (44)$$

which for sufficiently large R relative to δ (i.e., $h^+(\sqrt{2}\delta/R) \cong 1$) becomes

$$I(R) = \frac{\left(\frac{1}{(h^+(\delta))^2 R} + \frac{2}{h^+(\delta)}\right) \left(\frac{2N-1}{N}\right) + R}{4 + 2\sqrt{2}} \left(\frac{N}{N-2}\right) \left(\frac{N}{N-1}\right)^2 \quad (45)$$

Once again we see in Figs. 6 and 7 the same dependence on N as before approaching

$$I(R) = \frac{2 \left(\frac{1}{(h^+(\delta))^2 R} + \frac{2}{h^+(\delta)}\right) + R}{4 + 2\sqrt{2}} \quad (46)$$

in the limit as $N \rightarrow \infty$. We also note that whereas in the previous figures, for a given value of R , the improvement factor decreased with increasing frequency uncertainty, here it increases, which is consistent with Eq. (46) since, from Eq. (42), $h^+(\delta)$ is a monotonically decreasing function of δ . The intuitive reason for this occurrence is that, for the conventional SSME, the performance degrades much more severely in the presence of large frequency uncertainty than for the improved SSME since for the former the degradation factor $h^+(\delta)$ operates out on its tail whereas for the latter the effective frequency uncertainty is reduced by a factor of L and, thus, for large L the degradation factor $h^+(\delta/L) \cong h(\sqrt{2}\delta/R)$ operates near its peak of unity. Eventually for sufficiently large R , the improvement approaches $I(R) = R/(4 + 2\sqrt{2})$ as in Case 1. Finally, comparing Figs. 6 and 7 with Figs. 4 and 5, we observe that much larger frequency uncertainties can be tolerated for Case 2b than for Case 1.

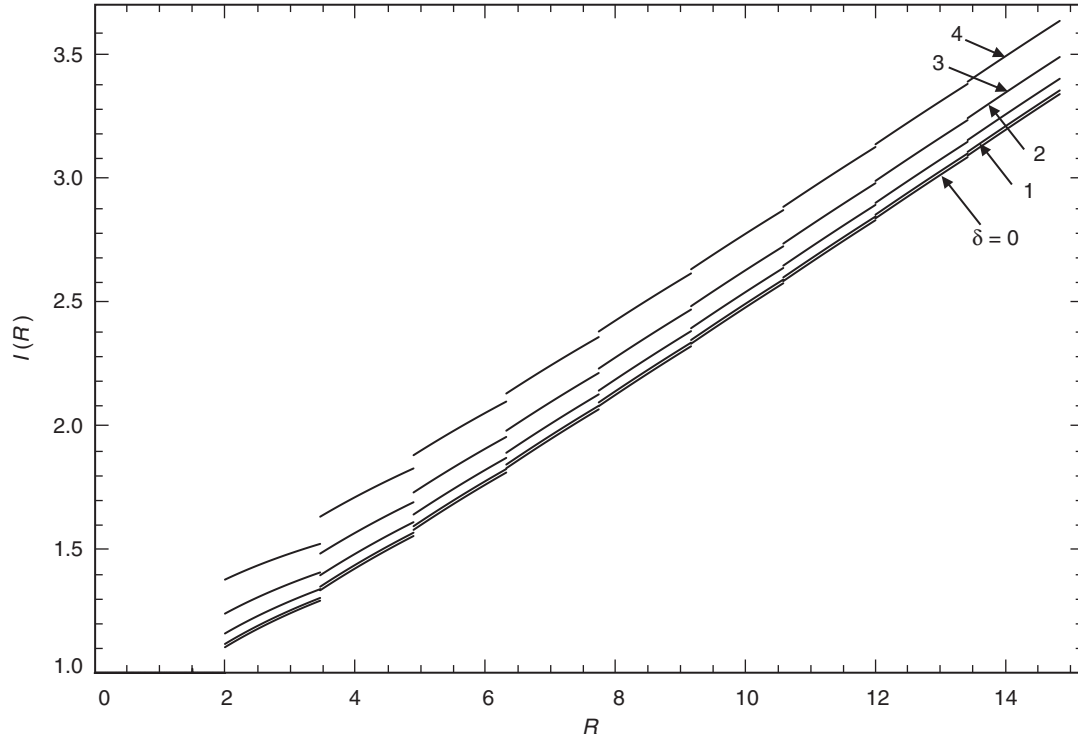


Fig. 6. Improvement factor versus SNR with normalized frequency uncertainty as a parameter; Case 2b; $N = 20$.

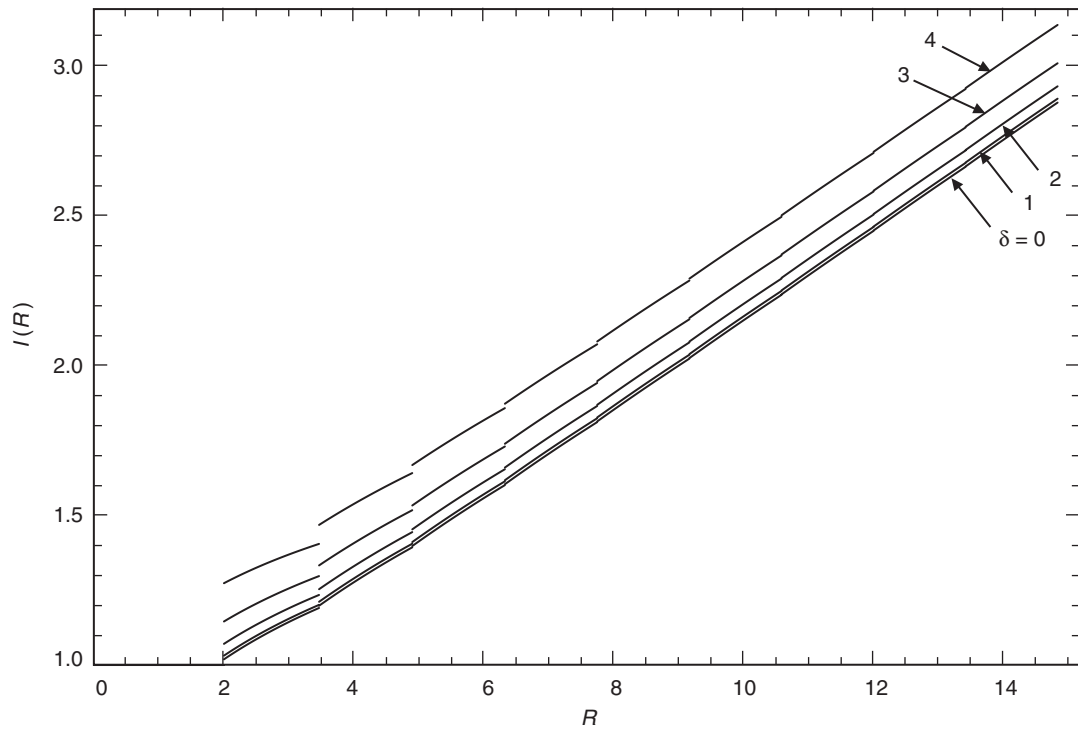


Fig. 7. Improvement factor versus SNR with normalized frequency uncertainty as a parameter; Case 2b; $N = 100$.

VII. Conclusions

We have demonstrated that the performance (as measured by its variance) of a popular SNR estimator can be improved by increasing the number of observables per symbol (accomplished by partitioning the symbol interval into a larger (than two) even number of subdivisions) but still processing them in successive pairs. We have shown that the amount of improvement is a function of the true SNR being estimated and continues to increase monotonically with increasing SNR. Despite its ad hoc nature, the modified estimator tracks the Cramer–Rao bound on the variance of SNR estimators with known or unknown data over the entire range of SNR values, a property not previously achievable with the conventional version of this estimator.

References

- [1] C. E. Gilchrist, “Signal-to-Noise Monitoring,” *JPL Space Programs Summary*, vol. IV, no. 37-27, pp. 169–184, June 1966.
- [2] C. M. Thomas, *Maximum Likelihood Estimation of Signal-to-Noise Ratio*, Ph.D. Dissertation, University of Southern California, Los Angeles, California, 1967.
- [3] R. M. Gagliardi and C. M. Thomas, “PCM Data Reliability Monitoring Through Estimation of Signal-to-Noise Ratio,” *IEEE Transactions on Communication*, vol. COM-16, pp. 479–486, June 1968.
- [4] E. A. Newcombe and S. Pasupathy, “Error Rate Monitoring for Digital Communications,” *Proceedings of the IEEE*, vol. 70, pp. 805–828, August 1982.
- [5] R. Matzner and F. Engleberger, “An SNR Estimation Algorithm Using Fourth-Order Moments,” *Proceedings of the IEEE International Symposium on Information Theory*, Trondheim, Norway, p. 119, June 1994.
- [6] D. R. Pauluzzi and N. C. Beaulieu, “A Comparison of SNR Estimation Techniques for the AWGN Channel,” *IEEE Transactions on Communication*, vol. 48, no. 10, pp. 1681–1691, October 2000.
- [7] M. K. Simon and A. Mileant, “SNR Estimation for the Baseband Assembly,” *The Telecommunications and Data Acquisition Progress Report 42-85, January–March 1986*, Jet Propulsion Laboratory, Pasadena, California, pp. 118–126, May 15, 1986. http://tmo.jpl.nasa.gov/tmo/progress_report/42-85/85K.PDF
- [8] B. Shah and S. Hinedi, “The Split Symbol Moments SNR Estimator in Narrow-Band Channels,” *IEEE Transactions on Aerospace Electronic Systems*, vol. AES-26, pp. 737–747, September 1990.
- [9] S. Dolinar, “Exact Closed-Form Expressions for the Performance of the Split-Symbol Moments Estimator of Signal-to-Noise Ratio,” *The Telecommunications and Data Acquisition Progress Report 42-100, October–December 1989*, Jet Propulsion Laboratory, Pasadena, California, pp. 174–179, February 15, 1990. http://tmo.jpl.nasa.gov/tmo/progres_report/42-100/100N.PDF
- [10] Y. Feraia, “A Complex Symbol Signal-to-Noise Ratio Estimator and Its Performance,” *The Telecommunications and Data Acquisition Progress Report 42-116, October–December 1993*, Jet Propulsion Laboratory, Pasadena, California, pp. 232–245, February 15, 1994. http://tmo.jpl.nasa.gov/tmo/progress_report/42-116/116s.pdf

- [11] M. K. Simon and S. Dolinar, "Signal-to-Noise Ratio Estimation for Autonomous Receiver Operation," to be presented at GLOBECOM 2004, Dallas, Texas, November 29–December 3, 2004.
- [12] H. L. Van Trees, *Detection, Estimation, and Modulation Theory*, vol. 1, New York: Wiley, 1968.
- [13] S. J. Dolinar, "Cramer-Rao Bounds for Signal-to-Noise Ratio and Combiner Weight Estimation," *The Telecommunications and Data Acquisition Progress Report 42-86, April–June 1986*, Jet Propulsion Laboratory, Pasadena, California, pp. 124–130, August 15, 1986.
http://tmo.jpl.nasa.gov/tmo/progress_report/42-86/86N.PDF